Scientific paper

Methyl Maltolate and Ethyl Maltolate Coordinated Oxidovanadium(V) Complexes with N'-(2-Hydroxy-5-methylbenzylidene)-4-trifluoromethylbenzohydrazide: Synthesis, Crystal Structures and Catalytic Epoxidation Property

Zhongduo Xiong^{1,2} and Ping Zhang^{1,2,*}

¹ Analysis and Testing Center, Wuhan Textile University, Wuhan 430073, P. R. China

² National Local Joint Laboratory for Advanced Textile Processing and Clean Production, Wuhan Textile University, Wuhan 430073, P. R. China

* Corresponding author: E-mail: sobear521@sohu.com

Received: 11-29-2022

Abstract

A mononuclear methyl maltolate (Hmm) coordinated oxidovanadium(V) complex [VOL¹(mm)] (1), and a mononuclear ethyl maltolate (Hem) coordinated oxidovanadium(V) complex [VOL²(em)] (2), where L¹ and L² are the dianionic form of N'-(2-hydroxy-5-methylbenzylidene)-3-trifluoromethylbenzohydrazide (H₂L¹) and N'-(2-hydroxy-5-methylbenzylidene)-4-trifluoromethylbenzohydrazide (H₂L²), respectively, have been prepared. The hydrazones and the complexes were characterized by elemental analysis, FT-IR and UV-Vis spectra. Structures of H₂L¹ and the two complexes were further characterized by single crystal X-ray diffraction. The two complexes have similar structures, with the V atoms in octahedral coordination. The hydrazones behave as ONO tridentate ligands with the V atoms. Both complexes have interesting properties on the catalytic epoxidation of cyclooctene.

Keywords: Hydrazone; oxidovanadium complex; mononuclear complex; crystal structure; catalytic epoxidation property

1. Introduction

Vanadium is an interesting element in various biological systems. Vanadium haloperoxidases are enzymes catalyzing the oxidation of halides to hypohalous acids, which then form oxygen. The enzymes can catalyze cyclization of terpene substrates, and the oxidation of sulfides to sulfoxides.2 Oxidation reaction is one of the most important reaction types in organic chemistry and chemical industry. However, without catalysts most oxidation processes are difficult. A deeper understanding of the catalytic functions of vanadium haloperoxidases prompted the synthesis and investigation of small molecule models for the active sites of these enzymes. In recent years, transition metal complexes with different ligands have been used as heterogeneous or homogenous or catalysts in the catalytic oxidation of organic substrates and in bioinorganic modeling of oxygen transfer metalloenzymes.³ Among the metal complexes, those with Schiff bases as ligands have

received particular attention because of their facile synthesis and wide application in the fields of biological, catalytic and magnetic.⁴ Vanadium complexes have been proved to show effective catalytic capability in the oxidation reactions of olefins and sulfides.⁵ Methyl maltol and ethyl maltol are food additive. In recent years, limited work has been reported that maltolate coordinated vanadium and molybdenum complexes have catalytic properties.⁶ The colleague of our research group has reported some vanadium complexes with catalytic properties.⁷ Aiming at obtaining new and efficient catalysts for the epoxidation of olefins, in this work, two new oxidovanadium(V) complexes, $[VOL^1(mm)]$ (1) and $[VOL^2(em)]$ (2), where L^1 and L^2 are the dianionic form of N'-(2-hydroxy-5-methylbenzylidene)-3-trifluoromethylbenzohydrazide (H₂L¹) and N'-(2-hydroxy-5-methylbenzylidene)-4-trifluoromethylbenzohydrazide (H₂L²), respetively (Scheme 1), and mm is methyl maltolate, em is ethyl maltolate, are presented.

Scheme 1. The hydrazones H_2L^1 and H_2L^2 .

2. Experimental

2. 1. Materials and Methods

5-Methylsalicylaldehyde, 3-trifluoromethylbenzohydrazide, 4-trifluoromethylbenzohydrazide and VO(acac)2 were purchased from Alfa Aesar and used as received. Methyl maltol and ethyl maltol were obtained from Aladin Chemical Co. Ltd. Reagent grade solvents were used as received. Microanalyses of the complexes were performed with a Vario EL III CHNOS elemental analyzer. Infrared spectra were recorded as KBr pellets with an FTS-40 spectrophotometer. Electronic spectra were recorded on a Lambda 900 spectrometer. ¹H NMR and ¹³C NMR spectra were recorded on a 500 MHz Bruker Advance instrument. The catalytic reactions were followed by gas chromatography on an Agilent 6890A chromatograph equipped with an FID detector and a DB5-MS capillary column (30 m × 0.32 mm, 0.25 μm). The X-ray powder diffraction patterns of the complexes were recorded on a Bruker AXS D8 Advance diffractometer.

Synthesis of N'-(2-hydroxy-5-methylbenzylidene)-3-trifluoromethylbenzohydrazide (H_2L^1)

5-Methylsalicylaldehyde (10 mmol, 1.36 g) and 3-trifluoromethylbenzohydrazide (10 mmol, 2.04 g) were refluxed in methanol (50 mL). The reaction was continued for 1 h in oil bath during which a solid compound separated. It was filtered and washed with cold methanol. The crude product was recrystallized from methanol and dried over anhydrous CaCl₂. Yield: 2.7 g (84%). IR data (KBr pellet, cm⁻¹): 3197 ν (N-H), 1649 ν (C=O), 1612 ν (C=N). UV-Vis data in methanol (nm): 218, 290, 300, 337, 433. Analysis: Found: C 59.45, H 4.14, N 8.76%. Calculated for C₁₆H₁₃F₃N₂O₂: C 59.63, H 4.07, N 8.69%. ¹H NMR $(d_6\text{-DMSO}, 500 \text{ MHz}) \delta \text{ (ppm)}: 12.22 \text{ (s, 1H, N}H), 10.87$ (s, 1H, OH), 8.63 (s, 1H, CH=N), 8.28 (s, 1H, ArH), 8.25 (d, 1H, ArH), 7.98 (d, 1H, ArH), 7.80 (t, 1H, ArH), 7.39 (s, 1H, ArH), 7.12 (d, 1H, ArH), 6.85 (d, 1H, ArH), 2.26 (s, 3H, CH₃). ¹³C NMR (d_6 -DMSO, 126 MHz) δ (ppm): 161.32, 155.30, 150.49, 148.54, 133.84, 132.27, 131.83, 129.87, 129.03, 128.42, 127.94, 124.10, 122.82, 118.37, 116.27, 19.91. Single crystals suitable for X-ray diffraction

were obtained by slow evaporation of the methanol solution containing the compound.

Synthesis of N'-(2-hydroxy-5-methylbenzylidene)-4-trifluoromethylbenzohydrazide (H,L²)

This compound was prepared by similar method as described for $\rm H_2L^1$, with 3-trifluoromethylbenzohydrazide replaced by 4-trifluoromethylbenzohydrazide (10 mmol, 2.04 g). Yield: 2.8 g (87%). IR data (KBr pellet, cm⁻¹): 3201 ν (N–H), 1657 ν (C=O), 1614 ν (C=N). UV-Vis data in methanol (nm): 220, 290, 301, 339, 435. Analysis: Found: C 59.52, H 4.16, N 8.62%. Calculated for $\rm C_{16}H_{13}F_3N_2O_2$: C 59.63, H 4.07, N 8.69%. ¹H NMR (d_6 -DMSO, 500 MHz) δ (ppm): 12.24 (s, 1H, NH), 10.91 (s, 1H, OH), 8.63 (s, 1H, CH=N), 8.15 (d, 2H, ArH), 7.93 (d, 2H, ArH), 7.38 (s, 1H, ArH), 7.11 (d, 1H, ArH), 6.85 (d, 1H, ArH), 2.25 (s, 3H, CH₃). ¹³C NMR (d_6 -DMSO, 126 MHz) δ (ppm): 161.62, 155.34, 148.78, 136.69, 132.26, 131.79, 131.53, 129.17, 128.54, 127.93, 125.49, 118.30, 116.27, 19.87.

Synthesis of the Complex [VOL¹(mm)] (1)

The hydrazone H_2L^1 (1.0 mmol, 0.32 g), methyl maltol (1.0 mmol, 0.13 g) and VO(acac)₂ (1.0 mmol, 0.26 g) were refluxed in methanol (30 mL). The reaction was continued for 1 h in oil bath to give a deep brown solution. Single crystals of the complex were formed during slow evaporation of the reaction mixture in air. The crystals were isolated by filtration, washed with cold methanol and dried over anhydrous CaCl2. Yield: 0.27 g (53%). IR data (KBr pellet, cm⁻¹): 1607 ν (-C=N-N=C-), 1264 ν (C-O_{phe}nolate), 1133 v(N-N), 972 v(V=O). UV-Vis data in methanol (nm): 247, 272, 325, 408. Analysis: Found: C 51.41, H 3.26, N 5.54%. Calculated for C₂₂H₁₆F₃N₂O₆V: C 51.58, H 3.15, N 5.47%. ¹H NMR (d_6 -DMSO, 500 MHz) δ (ppm): 9.20 (s, 1H, MMH), 8.43 (s, 1H, CH=N), 8.14 (s, 1H, ArH), 8.12 (d, 1H, ArH), 7.93 (d, 1H, ArH), 7.73 (t, 1H, ArH), 7.62 (s, 1H, ArH), 7.42 (d, 1H, ArH), 6.80 (d, 1H, ArH), 6.68 (d, 1H, MMH), 2.33 (s, 3H, CH₃), 2.24 (s, 3H, CH₃). ¹³C NMR (d_6 -DMSO, 126 MHz) δ (ppm): 175.54, 167.77, 161.71, 158.37, 157.96, 155.59, 145.81, 136.63, 134.24, 132.65, 131.95, 130.86, 130.19, 129.92, 129.53, 128.15, 124.90, 122.73, 118.90, 118.14, 19.87, 15.08.

Synthesis of the Complex $[VOL^2(em)]$ (2)

This complex was prepared by similar method as described for 1, with H_2L^1 replaced by H_2L^2 (1.0 mmol, 0.32 g), and with methyl maltol replaced by ethyl maltol (1.0 mmol, 0.14 g). Yield: 0.25 g (48%). IR data (KBr pellet, cm⁻¹): 1607 ν (-C=N-N=C-), 1268 ν (C-O_{phenolate}), 1124 ν (N-N), 969 ν (V=O). UV-Vis data in methanol (nm): 255, 270, 325, 412. Analysis: Found: C 52.61, H 3.38, N 5.40%. Calculated for $C_{23}H_{18}F_3N_2O_6V$: C 52.48, H 3.45, N 5.32%. ¹H NMR (d_6 -DMSO, 500 MHz) δ (ppm): 9.18 (s, 1H, EMH), 8.45 (s, 1H, CH=N), 8.06 (d, 2H, ArH), 7.83 (d, 2H, ArH), 7.65 (s, 1H, ArH), 7.43 (d, 1H,

Ar*H*), 6.82 (d, 1H, Ar*H*), 6.68 (d, 1H, MM*H*), 2.33 (s, 3H, C*H*₃), 2.13 (q, 2H, C*H*₂), 1.13 (t, 3H, C*H*₃). ¹³C NMR (d_6 -DMSO, 126 MHz) δ (ppm): 175.78, 167.56, 161.83, 158.47, 155.69, 154.70, 153.20, 136.68, 134.58, 133.67, 133.19, 130.08, 129.91, 128.80, 125.65, 124.35, 118.92, 115.58, 21.30, 20.78, 10.81.

2. 2. Crystal Structure Determination

Data were collected on a Bruker SMART 1000 CCD area diffractometer using a graphite monochromator Mo $K\alpha$ radiation ($\lambda = 0.71073$ Å) at 298(2) K. The data were corrected with SADABS programs and refined on F^2 with SHELXL software. Structures of H₂L¹ and the complexes were solved by direct methods and difference Fourier syntheses. All non-hydrogen atoms were refined anisotropically. The N and O attached H atoms were located from a difference Fourier map and refined with N-H and O-H distances restrained to 0.90(1) and 0.85(1) Å, respectively. The remaining hydrogen atoms were placed in calculated positions and included in the last cycles of refinement. The trifluoromethyl groups in H₂L¹ and complex 1 are disordered over two sites, with occupancies of 0.55(1) and 0.45(1), and 0.71(1) and 0.29(1), respectively. Crystal data and details of the data collection and refinement are listed in Table 1.

2. 3. Catalytic Epoxidation Process

A mixture of cyclooctene (2.76 mL, 20 mmol), acetophenone (internal reference) and the complex as the catalyst (0.05 mmol) was stirred and heated up to 80 °C before addition of aqueous tert-butyl hydroperoxide (TBHP; 70% w/w, 5.48 mL, 40 mmol). The mixture is initially an emulsion, but two phases become clearly visible as the reaction progresses, a colorless aqueous one and a colorful organic one. The reaction was monitored for 5 h with withdrawal and analysis of organic phase aliquots (0.1 mL) at required times. Each withdrawn sample was mixed with 2 mL of diethylether, treated with a small quantity of MnO₂ and then filtered through silica and analyzed by GC.

3. Results and Discussion

3. 1. Synthesis

The hydrazones H_2L^1 and H_2L^2 were prepared from 5-methylsalicylaldehyde with 3-trifluoromethylbenzohydrazide and 4-trifluoromethylbenzohydrazide, respectively, in methanol. The two complexes were facile prepared by the hydrazones with $VO(acac)_2$ in the presence of methyl maltol and ethyl maltol, respectively (Scheme 2).

Parameters	H_2L^1	1	2
Empirical formula	$C_{16}H_{13}F_3N_2O_2$	C ₂₂ H ₁₆ F ₃ N ₂ O ₆ V	C ₂₃ H ₁₈ F ₃ N ₂ O ₆ V
Formula weight	322.28	512.31	526.33
Crystal system	Monoclinic	Monoclinic	Triclinic
Space group	$P2_1/c$	$P2_1/c$	P-1
a [Å]	11.7599(7)	12.163(1)	7.503(1)
<i>b</i> [Å]	15.0697(8)	7.652(1)	11.877(1)
c [Å]	8.7575(4)	24.871(2)	13.302(1)
α [°]	90	90	107.289(1)
β [°]	95.259(1)	100.430(1)	93.212(1)
, γ [°]	90	90	90.773(1)
V [Å ³]	1545.45(14)	2276.5(4)	1129.5(2)
Z	4	4	2
$\rho_{\rm calcd.}$ [g cm ⁻³]	1.385	1.495	1.548
$\mu [\mathrm{mm}^{-1}]$	0.117	0.501	0.507
F(000)	664	1040	536
Index ranges	$-14 \le h \le 14$	$-14 \le h \le 14$	$-6 \le h \le 9$
	$-18 \le k \le 18$	$-7 \le k \le 9$	$-10 \le k \le 14$
	$-10 \le l \le 10$	$-30 \le l \le 28$	$-16 \le l \le 16$
Measured reflections	16591	12860	6007
Independent reflections	2876	4244	4154
Observed reflections ($I > 2\sigma(I)$)	2192	2423	2751
Parameters	243	341	316
Restraints	50	54	18
Final R indices $[I > 2\sigma(I)]$	0.0437, 0.1110	0.0788, 0.2237	0.0507, 0.1144
R indices (all data)	0.0596, 0.1234	0.1359, 0.2663	0.0905, 0.1355
Goodness-of-fit on F^2	1.012	1.041	1.029

Scheme 2. The synthesis procedure of the hydrazones and the complexes. H_2L^1 : $X = CF_3$, Y = H; H_2L^2 : X = H, $Y = CF_3$; 1: $X = CF_3$, Y = H, Z = Me; 2: X = H, $Y = CF_3$, Z = Et.

The hydrazones behave as tridentate dianionic ONO donor ligands toward the VO^{3+} core. The two complexes were synthesized by the reaction of the hydrazones with $VO(acac)_2$ in the presence of methyl maltol or ethyl maltol, in 1:1:1 molar proportion in methanol under reflux. Both H_2L^1 and the vanadium complexes were isolated as single crystals from the reaction mixtures by slow evaporation method at room temperature. Crystals of H_2L^1 and the complexes are fairly soluble in most organic solvents like ethanol, methanol, acetonitrile, DMF and DMSO.

The experimental powder X-ray diffraction (XRD) patterns of the bulk samples of both complexes agree well

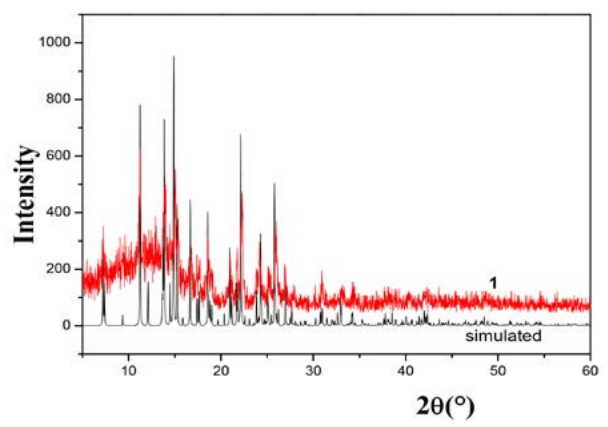


Figure 1. Experimental and simulated powder XRD patterns of complex 1.

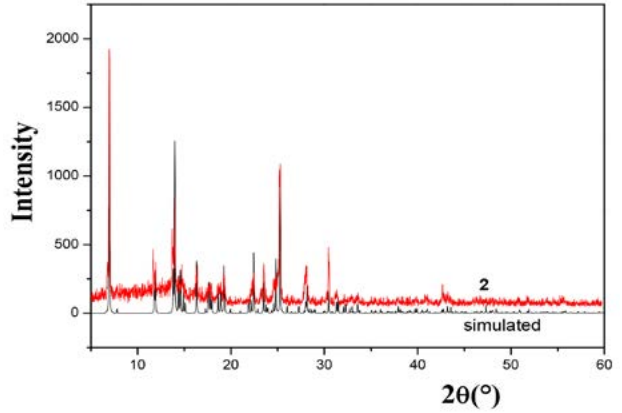


Figure 2. Experimental and simulated powder XRD patterns of complex 2.

with the simulated patterns calculated from single crystal X-ray diffraction (Figures 1 and 2).

3. 2. IR and Electronic Spectra

The infrared spectra of the hydrazones show weak bands centered at about 3200 cm⁻¹ for ν (N-H) and 1649-1657 cm⁻¹ for ν (C=O).8 On complexation the absence of N-H and C=O bands and red shifts in azomethine (-C=N-N=C-) bands of the ligands show coordination of the hydrazones in the enol form. The infrared spectra of the complexes display IR absorption bands at 1607 cm⁻¹ which can be assigned to the C=N stretching frequency of the coordinated hydrazone ligands whereas for the free hydrazones the same bands are observed at 1612-1614 cm⁻¹.¹⁰ The vanadium complexes exhibit characteristic bands at about 970 cm⁻¹ for the stretching vibrations of the V=O bonds. 11 Based on the infrared absorption, it is clear that the hydrazones exist in keto-amino tautomer form in free, and in imino-enol tautomeric form in the vanadium complexes.12

Electronic spectra of both vanadium complexes recorded in methanol show weak absorption bands centered at about 410 nm, which can be assigned to charge transfer transitions of N($p\pi$)–M($d\pi$) LMCT. The medium absorption bands centered at 320 nm for the vanadium complexes are assigned as charge transfer transitions of O($p\pi$)–M($d\pi$) LMCT, which is similar to that reported in literature.¹³

3. 3. Description of the Structure of H_2L^1

The perspective view of the hydrazone H_2L^1 is shown in Figure 3. Selected bond lengths and angles are listed in Table 1. The hydrazone molecule presents in E conformation with respect to the C=N double bond. The dihedral angles between the mean planes of the central N-N=C spacer unit and the C1-C6 and C9-C14 benzene rings are 20.3(3) and 9.3(3)°, respectively, while the dihedral angle between the two aromatic rings is 12.2(4)°. An intra-molecular N-H···O hydrogen bond makes an S(6) ring motif. In the crystal of the compound, the molecules are linked by N-H···O and C-H···O hydrogen bonds (Table 2), to form one-dimensional chain along the c axis (Figure 4). The molecules are further linked by three π ··· π stacking

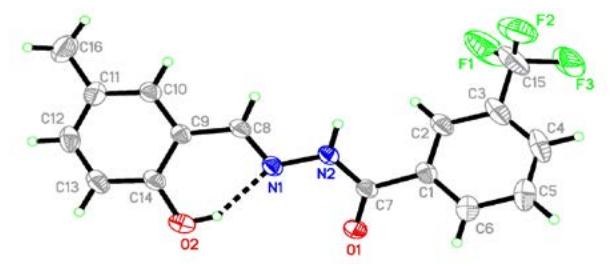


Figure 3. ORTEP plots (30% probability level) and numbering scheme for H_2L^1 .

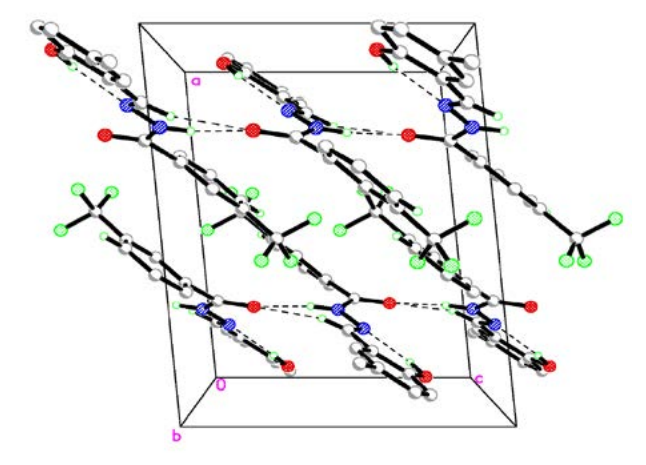


Figure 4. The molecular packing diagram of H_2L^1 , viewed down the b axis. Hydrogen bonds are shown as dashed lines.

interactions involving pairs of benzene rings with the ring-centroid separations of 3.806–4.147 Å.

3. 4. Description of the Structures of the Complexes

The perspective views of the vanadium complexes 1 and 2 are shown in Figures 5 and 6, respectively. In each complex, the V atom is in distorted octahedral coordination with NO₅ chromophore. The hydrazone compound behaves as dianionic tridentate ligand binding through the phenolate oxygen (O2), the enolate oxygen (O1) and the imine nitrogen (N1), and occupies three positions in the equatorial plane of the octahedral coordination. The fourth position of the equatorial plane is occupied by the deprotonated hydroxyl oxygen (O5) of the MM or EM ligand. The carbonyl oxygen (O4) of the MM or EM ligand occupies one axial position of the octahedral coordination, and the other axial position is defined by the oxido group (O3). The V atoms are found to be deviated from the mean equatorial planes defined by the four donor atoms by 0.308(1) Å for 1 and 0.293(1) Å for 2. The V-O4 bonds are longer than the typical single bonds (2.267(4) Å and 2.253(2) Å against 1.9-2.0 Å). This indicates that the carbonyl oxygen atom is loosely binds with the V atom. The V-O bonds (1.57-1.94 Å) and the V-N bonds (2.09-2.10

Å) are similar to those observed in other vanadium(V) complexes. 4e,14 The C7-O1 bonds in both complexes are 1.299(6) Å and 1.322(4) Å, respectively, which are longer than that in the free hydrazone H₂L¹, and are closer to single bonds rather than double bonds. The shorter bond lengths compared to C-O single bond may be due to extended electron delocalization in the hydrazone ligands. 15 Moreover, the shortening of C7–N2 bonds (1.28–1.29 Å, instead of 1.34 Å in H₂L¹) and the elongation of N1–N2 bonds (1.39-1.41 Å) also prove the electron cloud delocalization in the hydrazone ligand systems. The hydrazones bind with the V atoms through five- and six-membered chelate rings. The five-membered rings are rather planar, while the six-membered rings are obviously distorted. The two benzene rings form dihedral angles of 5.1(4)° for 1 and 2.8(5)° for 2. The *trans* angles in both complexes are in the range 153.1(2)-174.5(2)°, indicating the distortion of the octahedral coordination.

In the crystal structure of complex **1**, the complex molecules are linked by C–H···O hydrogen bonds (Table 2), to form 1D chain running along the b-axis (Figure 7). The molecules are further linked by five π ··· π stacking interactions involving pairs of V-O1-C7-N2-N1, V-O4-C19-C18-O5, O6-C17-C18-C19-C20-C21 and C1-C2-C3-C4-C5-C6 rings with the ring-centroid separations of 2.826–4.850 Å. In the crystal packing diagram of complex

Table 2. Selected Bond Lengths (Å) and Angles (°) for $\mathrm{H}_2\mathrm{L}^1$ and the Complexes

	H_2L^1	1	2
V-O1		1.929(4)	1.937(2)
V-O2		1.831(4)	1.837(3)
V-O3		1.582(5)	1.582(3)
V-O4		2.264(4)	2.253(2)
V-O5		1.857(4)	1.867(2)
V-N1		2.088(5)	2.100(3)
C8-N1	1.279(3)	1.285(8)	1.281(4)
N2-C7	1.340(3)	1.300(8)	1.289(4)
N1-N2	1.388(2)	1.391(6)	1.392(4)
C7-O1	1.227(2)	1.294(7)	1.322(4)
O3-V-O2		101.3(2)	100.8(2)
O3-V-O5		99.2(2)	98.2(1)
O2-V-O5		99.9(2)	98.9(1)
O3-V-O1		97.2(2)	95.0(1)
O2-V-O1		153.1(2)	155.5(1)
O5-V-O1		96.2(2)	97.3(1)
O3-V-N1		99.2(2)	101.2(1)
O2-V-N1		83.3(2)	83.6(1)
O5-V-N1		160.3(2)	159.7(1)
O1-V-N1		74.6(2)	75.0(1)
O3-V-O4		174.7(2)	173.5(1)
O2-V-O4		83.4(2)	84.7(1)
O5-V-O4		77.4(2)	77.5(1)
O1-V-O4		79.3(2)	80.9(1)
N1-V-O4		83.6(2)	82.7(1)

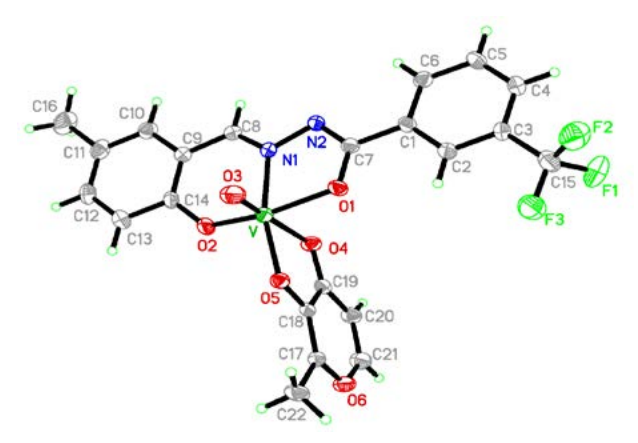


Figure 5. ORTEP plots (30% probability level) and numbering scheme for complex **1**.

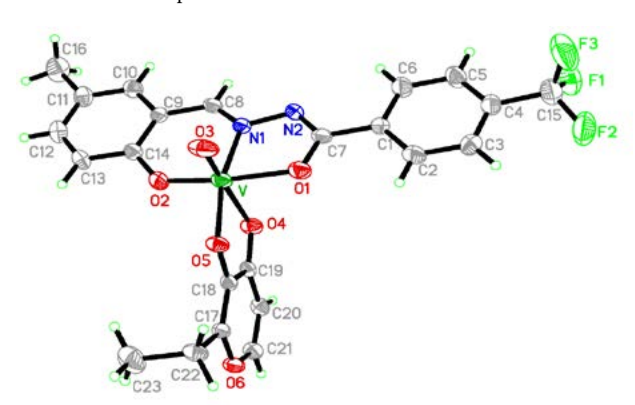


Figure 6. ORTEP plots (30% probability level) and numbering scheme for complex **2**.

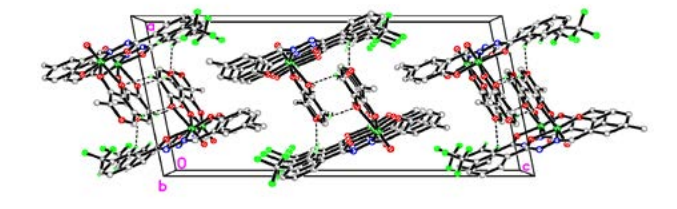


Figure 7. The molecular packing diagram of complex 1, viewed down the b axis. Hydrogen bonds are shown as dashed lines.

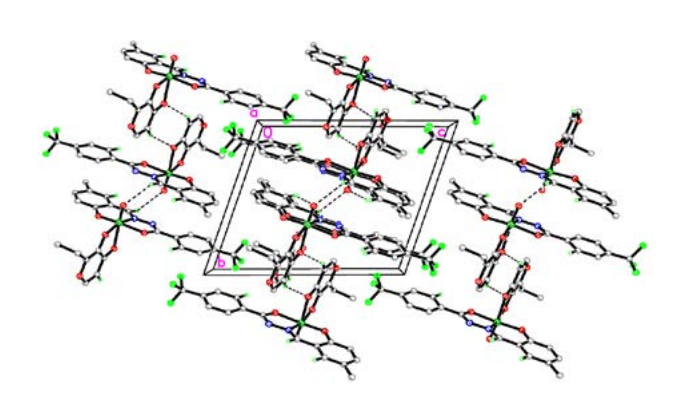


Figure 8. The molecular packing diagram of complex 2, viewed down the b axis. Hydrogen bonds are shown as dashed lines.

2, the molecules are linked by C–H···O hydrogen bonds (Table 2), to form 1D chain running along the b-axis (Figure 8). The molecules are further linked by nine π ··· π stacking interactions involving pairs of V-O1-C7-N2-N1, V-O4-C19-C18-O5, V-O2-C14-C9-C8-N1, O6-C17-C18-C19-C20-C21 and C9-C10-C11-C12-C13-C14 rings with the ring-centroid separations of 2.856–4.951 Å.

Table 3. Hydrogen Bond Distances (Å) and Bond Angles (°) for H_2L^1 and the Complexes

D-H··· A $d(D$ -H)	$d(H\cdots A)$	$d(D\cdots A)$	Angle (D	P−H··· <i>A</i>)
$\overline{H_2L^1}$				
O2-H2A···N1	0.86(1)	1.90(2)	2.665(2)	148(4)
N2-H2B···O1i	0.90(1)	1.99(2)	2.879(2)	165(4)
C8-H8···O1i	0.93	2.52(2)	3.263(3)	138(5)
1				
C2-H2···O6 ⁱⁱ	0.93	2.50(2)	3.315(3)	147(5)
C20-H20···O4 ⁱⁱⁱ	0.93	2.52(2)	3.316(3)	143(5)
2				
C2-H2···O6 ^{iv}	0.93	2.60(3)	3.429(4)	149(6)
C8-H8···O3 ^v	0.93	2.54(3)	3.133(4)	122(5)
C10-H10···O3 ^{vi}	0.93	2.52(3)	3.390(5)	156(6)
C20-H20···O4 ^{vii}	0.93	2.46(3)	3.287(4)	149(65)

Symmetry codes: i): x, 1/2 - y, -1/2 + z; ii): 1 - x, 1 - y, -z; iii): 1 - x, 2 - y, -z; iv): 1 - x, -y, 1 - z; v): 2 - x, 1 - y, 1 - z; vi): 1 + x, y, z; vii): 2 - x, -y, 1 - z.

3. 5. Catalytic Epoxidation Results

Before addition of aqueous TBHP at 80 °C, the two vanadium complexes were dissolved in the organic phase. Since the organic phase was colorful and the aqueous phase was colorless, both complexes are mainly confined in the organic phase. Moreover, TBHP was mainly transferred into the organic phase under this condition. Cyclooctene oxide and cyclooctene are poorly soluble in water, so the determination of the epoxide selectivity (epox-

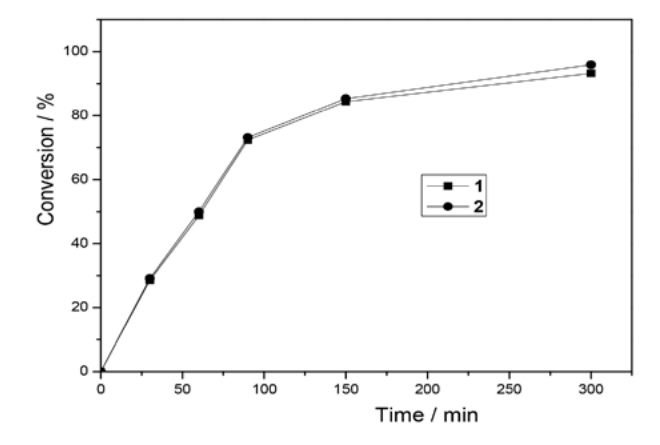


Figure 9. Kinetic monitoring of *cis*-cyclooctene epoxidation with TBHP–H₂O in the presence of the complexes.

ide formation/cyclooctene conversion) is expected to be accurate. The present study indicates effective property for the cyclooctene epoxidation by using aqueous TBHP. Kinetic profiles of both complexes are shown in Figure 9. The cyclooctene conversions of the two complexes are similar before 90 min of the reaction. After 90 min, complex 2 is a little better than complex 1. The cyclooctene conversion is 93% for 1 and 96% for 2 at 5 h, and the selectivity toward cyclooctene oxide is 75% for 1 and 77% for 2. The catalytic properties of the present two complexes are similar to the vanadium and molybdenum complexes reported in literature. ¹⁶

4. Conclusion

Two new methyl maltolate and ethyl maltolate coordinated oxidovanadium(V) complexes derived from similar tridentate hydrazone ligands N-(2-hydroxy-5-methylbenzylidene)-3-trifluoromethylbenzohydrazide and N-(2-hydroxy-5-methylbenzylidene)-4-trifluoromethylbenzohydrazide were prepared. The hydrazone ligands coordinate to the V atoms through the ONO donor set. The maltolate ligands coordinate to the V atoms through the carbonyl and phenolate O atoms. The V atoms in both complexes are in octahedral coordination. Both complexes have effective catalytic epoxidation properties on cyclooctene.

Supplementary Data

CCDC numbers 2222502 (H₂L¹), 2222504 (1) and 2222505 for (2) contain the supplementary crystallographic data. These data can be obtained free of charge *via* http://www.ccdc.cam.ac.uk/conts/retrieving.html, or from the Cambridge Crystallographic Data Center, 12, Union Road, Cambridge CB2 1EZ, UK; fax: +44 1223 336 033; or e-mail: deposit@ccdc.cam.ac.uk.

Acknowledgments

This work was supported by the Collaborative Innovation Plan of Hubei Province for Key Technology of Eco-Ramie Industry.

5. References

- (a) J. B. Fournier, E. Rebuffet, L. Delage, R. Grijol, L. Meslet-Cladiere, J. Rzonca, P. Potin, G. Michel, M. Czjzek, C. Leblanc, Appl. Environ. Microbiol. 2014, 80, 7561–7573;
 - **DOI:**10.1128/AEM.02430-14 (b) G. J. Colpas, B. J. Hamstra, J. W. Kampf, V. L. Pecoraro, *J.*
 - **DOI:**10.1021/ja953791r

Am. Chem. Soc. 1996, 118, 3469-3478.

(a) T. S. Smith, V. L. Pecoraro, *Inorg. Chem.* 2002, 41, 6574–6760; DOI:10.1021/ja029271v

- (b) J. N. Carter-Franklin, J. D. Parrish, R. A. Tschirret-Guth, R. D. Little, A. Butler, *J. Am. Chem. Soc.* **2003**, *125*, 3688–3689.
- (a) T. Q. Liu, G. Li, N. N. Shen, L. Q. Wang, B. J. J. Timmer, A. Kravchenko, S. Y. Zhou, Y. Gao, Y. Yang, H. Yang, B. Xu, B. B. Zhang, M. S. G. Ahlquist, L. C. Sun, *Chem. Eur. J.* 2022, 28, e202104562;
 - (b) K. Moghe, A. K. Sutar, I. K. Kang, K. C. Gupta, *RSC Advances* **2019**, *9*, 30823–30834;

DOI:10.1039/C9RA05811G

- (c) Y. Lei, Acta Chim. Slov. 2022, 69, 235-242;
- (d) Q. B. Li, Y. J. Han, G. Q. Zhao, L. W. Xue, *Acta Chim. Slov.* **2017**, *64*, 500–505; **DOI**:10.17344/acsi.2017.3416
- (e) M. R. Maurya, N. Kumar, F. Avecilla, ACS Omega 2022, DOI:10.1021/acsomega.2c06732
- (f) P. Devi, M. Kannan, Kiran, Virender, A. Kumar, S. Muthai-ah, *J. Organomet. Chem.* **2022**, 980–981, 122515;

DOI:10.1016/j.jorganchem.2022.122515

- (g) K. S. Yu, Y. Sun, D. W. Zhu, Z. Y. Xu, J. Y. Wang, J. Y. Shen, Q. J. Zhang, W. Zhao, *Chem. Commun.* **2022**, *58*, 12835–12838; **DOI:**10.1039/D2CC04846A
- (h) R. K. Sahoo, S. Rajput, A. G. Patro, S. Nembenna, *Dalton Trans.* **2022**, *51*, 16009–16016. **DOI**:10.1039/D2DT02846H
- (a) T. A. Bazhenova, V. S. Mironov, I. A. Yakushev, R. D. Svetogorov, O. V. Maximova, Y. V. Manakin, A. B. Kornev, A. N. Vasiliev, E. B. Yagubskii, *Inorg. Chem.* 2020, 59, 563–578; DOI:10.1021/acs.inorgchem.9b02825
 - (b) S. K. Patel, K. Kolte, C. J. Savani, P. Raghavaiah, D. Dave, A. A. Isab, D. Mistry, D. Suthar, V. K. Singh, *Inorg. Chim. Acta* **2022**, *543*, 121139; **DOI**:10.1016/j.ica.2022.121139
 - (c) K. Kim, S. Nayab, Y. Cho, H. Jung, H. Yeo, H. Lee, S. H. Lee, RSC Advances **2023**, *12*, 35896–35904;

DOI:10.1039/D2RA07241F

- (d) K. Dankhoff, M. Gold, L. Kober, F. Schmitt, L. Pfeifer, A. Durrmann, H. Kostrhunova, M. Rothemund, V. Brabec, R. Schobert, B. Weber, *Dalton Trans.* **2019**, *48*, 15220–15230; **DOI**:10.1039/C9DT02571E
- (e) N. Ranjitha, G. Krishnamurthy, H. S. B. Naik, M. Pari, L. Afroz, K. R. Sumadevi, M. N. Manjunatha, *Inorg. Chim. Acta* **2022**, 543, 121191; **DOI:**10.1016/j.ica.2022.121191
- (g) E. Zarenezhad, S. Esmaielzadeh, *Acta Chim. Slov.* **2018**, 65, 416–428. **DOI**:10.17344/acsi.2018.4159
- (a) A. Mahdian, M. H. Ardakani, E. Heydari-Bafrooei, S. Saeednia, *Appl. Organomet. Chem.* 2021, 35, e6170;
 DOI:10.1002/aoc.6170
 - (b) P. Mokhtari, G. Mohammadnezhad, *Polyhedron* **2022**, *215*, 115655; **DOI:**10.1016/j.poly.2022.115655
 - (c) H. Hayashibara, X. H. Hou, K. Nomura, *Chem. Commun.* **2018**, 54, 13559–13562; **DOI:**10.1039/C8CC07974A
 - (d) M. Q. E. Mubarak, S. P. de Visser, *Dalton Trans.* **2019**, 48, 16899–16910; **DOI:**10.1039/C9DT03048D
 - (e) M. Liang, N. Sun, D.-H. Zou, Acta Chim. Slov. 2018, 65, 964–969; DOI:10.17344/acsi.2018.4625
 - (f) A. M. F. Phillips, H. Y. Suo, M. D. C. G. da Silva, A. J. L. Pombeiro, W. H. Sun, *Coord. Chem. Rev.* **2020**, *416*, 213332. **DOI:**10.1016/j.ccr.2020.213332

- 6. (a) D.-H. Zou, M. Liang, W. Chen, *Acta Chim. Slov.* **2021**, 68, 441–446; **DOI**:10.17344/acsi.2020.6553
 - (b) Y.-M. Cui, Y.-Q. Wang, X.-X. Su, H. Huan, P. Zhang, *J. Struct. Chem.* **2019**, *60*, 1299–1305;

DOI:10.1134/S0022476619080092

- (c) R. C. Maurya, P. Bohre, S. Sahu, M. H. Martin, A. K. Sharma, P. Vishwakarma, *Arab. J. Chem.* **2016**, 9, S150–S160. **DOI**:10.1016/j.arabjc.2011.02.027
- (a) Y.M. Cui, Y.Q. Wang, X.X. Su, H. Huan, P. Zhang, J. Struct. Chem. 2019, 60, 1299–1305;

DOI:10.1134/S0022476619080092

(b) Q.A. Peng, X.P. Tan, Y.D. Wang, S.H. Wang, Y.X. Jiang, Y.M. Cui, *Acta Chim. Slov.* **2020**, *67*, 644–650;

DOI:10.17344/acsi.2019.5650

- (c) Y.J. Cai, Y.Y. Wu, F. Pan, Q.A. Peng, Y.M. Cui, *Acta Chim. Slov.* **2020**, *67*, 896–903. **DOI:**10.17344/acsi.2020.5895
- 8. G. M. Sheldrick, SHELXS97 Program for solution of crystal structures, University of Göttingen, Germany, **1997**.
- (a) Y.-T. Ye, F. Niu, Y. Sun, D. Qu, X.-L. Zhao, J. Wang, D.-M. Xian, H. Jurg, Z.-L. You, Chinese J. Inorg. Chem. 2015, 31, 1019–1026;
 - (b) H.-Y. Qian, *Inorg. Nano-Met. Chem.* **2018**, 48, 615–619. **DOI**:10.1080/24701556.2019.1567542
- R. Bikas, V. Lippolis, N. Noshiranzadeh, H. Farzaneh-Bonab,
 A. J. Blake, M. Siczek, H. Hosseini-Monfared, T. Lis, *Eur. J. Inorg. Chem.* 2017, 6, 999–1006.

DOI:10.1002/ejic.201601359

- (a) R. A. Lal, M. Chakrabarty, S. Choudhury, A. Ahmed, R. Borthakur, A. Kumar, *J. Coord. Chem.* **2010**, *63*, 163–175;
 DOI:10.1080/00958970903259451
 - (b) T. Glowiak, L. Jerzykiewicz, J. A. Sobczak, J. J. Ziolkowski, *Inorg. Chim. Acta* **2003**, *356*, 387–392.

DOI:10.1016/S0020-1693(03)00301-3

- C. A. Koellner, N. A. Piro, W. S. Kassel, C. R. Goldsmith, C. R. Graves, *Inorg. Chem.* 2015, 54, 7139–7141.
 DOI:10.1021/acs.inorgchem.5b01136
- (a) A. Kumar, S. D. Kurbah, I. Syiemlieh, S. A. Dhanpat, R. Borthakur, R. A. Lal, *Inorg. Chim. Acta* 2021, 515, 120068;
 DOI:10.1016/j.ica.2020.120068
 (b) P. P. Patil, P. Javaranna, A. C. Kumar, N. Naik, *Chamis*.
 - (b) P. R. Patil, R. Javarappa, A. C. Kumar, N. Naik, *ChemistrySelect* 2022, 7, e202200752; DOI:10.1002/slct.202200752
 (c) J. Szklarzewicz, A. Jurowska, D. Matoga, K. Kruczala, G. Kazek, B. Mordyl, J. Sapa, M. Papiez, *Polyhedron* 2020, 185, 114589. DOI:10.1016/j.poly.2020.114589
- 14. (a) R. Hahn, U. Kusthardt, W. Scherer, *Inorg. Chim. Acta* 1993, 210, 177–182; DOI:10.1016/S0020-1693(00)83325-3
 (b) S. Gupta, A. K. Barik, S. Pal, A. Hazra, S. Roy, R. J. Butcher, S. K. Kar, *Polyhedron* 2007, 26, 133–141;
 - **DOI:**10.1016/j.poly.2006.08.001 (c) M. Bagherzadeh, M. Zare, V. Amani, A. Allern, L. K. Woo,

Polyhedron **2013**, *53*, 223–229. **DOI:**10.1016/j.poly.2013.01.054

- (a) L. Y. He, X. Y. Qiu, J. Y. Cheng, S. J. Liu, S. M. Wu, Polyhedron 2018, 156, 105–110; DOI:10.1016/j.poly.2018.09.017
 (b) T. M. Asha, M. R. P. Kurup, Polyhedron 2019, 169, 151–161; DOI:10.1016/j.poly.2019.04.045
 (c) Z. Q. Sun, S. F. Yu, X. L. Xu, X. Y. Qiu, S. J. Liu, Acta Chim. Slov. 2020, 67, 1281–1289. DOI:10.17344/acsi.2020.6236
- Y. M. Cui, W. T. Liu, W. X. Yan, Russ. J. Coord. Chem. 2019, 45, 222–229. DOI:10.1134/S1070328419030023
- (a) L. Liu, J. Liu, J. Liu, W. Chen, Y. Cui, Synth. React. Inorg. Met.-Org. Nano-Met. Chem. 2016, 46, 1871–1878;
 DOI:10.1080/15533174.2015.1137075
 - (b) Y. M. Cui, Y. Q. Wang, X. X. Su, H. Huang, P. Zhang, J. Struct. Chem. **2019**, 60, 1299–1305.

DOI:10.1134/S0022476619080092

Povzetek

Sintetizirali smo enojedrni oksidovanadijev(V) kompleks [VOL¹(mm)] (1) z ligandom metil maltolat (Hmm) in enojedrni oksidovanadijev(V) kompleks z etil maltolatom (Hem) [VOL²(em)] (2), pri čemer sta L^1 in L^2 dianionski obliki N^2 -(2-hidroksi-5-metilbenziliden)-3-trifluorometilbenzohidrazida (H_2L^1) in N^2 -(2-hidroksi-5-metilbenziliden)-4-trifluorometilbenzohidrazida (H_2L^2). Hidrazone in komplekse smo karakterizirali z elementno analizo, FT-IR in UV-Vis spektroskopijo. Strukture H_2L^1 in obeh kompleksov smo določili z monokristalno rentgensko difrakcijo. Oba kompleksa imata podobne strukture z oktaedrično koordiniranimi vanadijevimi atomi. Hidrazoni se na vanadij vežejo kot tridentatni ONO ligandi. Oba kompleksa kažeta zanimive katalitske lastnosti pri epoksidaciji ciklooktena.



Except when otherwise noted, articles in this journal are published under the terms and conditions of the Creative Commons Attribution 4.0 International License